Supplementary Material for 'Observed change and the extent of coherence in the Gulf Stream system'

Helene Asbjørnsen[1,2], Tor Eldevik[1,2], Johanne Skrefsrud[1,2], Helen L. Johnson[3], and Alejandra Sanchez-Franks[4]

[1]Geophysical Institute, University of Bergen, Bergen, Norway
[2]Bjerknes Centre for Climate Research, Bergen, Norway
[3]Department of Earth Sciences, University of Oxford, Oxford, United Kingdom
[4]National Oceanography Centre, Southampton, United Kingdom

Contents of this file

Table S 1. Coherence in ECCOv4-r4 when the Ekman layer (0-100m) is removed. Correlations (at zero lag time) between normalized, low-pass filtered transport time series ECCOv4-r4 (1992-2017). Significant correlations at the 95% confidence level in bold font (Chelton (1983) method).

	Florida Current	WBC	Oleander GS	OSNAP NAC	GSR	Svinøy	BSO
Florida Current	1	**0.90**	0.69	-0.36	-0.24	0.12	-0.46
WBC	-	1	**0.77**	-0.32	-0.44	-0.01	-0.65
Oleander GS	-	-	1	-0.25	-0.22	0.22	-0.58
OSNAP NAC	-	-	-	1	0.16	0.03	0.31
GSR	-	-	-	-	1	**0.65**	**0.62**
Svinøy	-	-	-	-	-	1	0.21
BSO	-	-	-	-	-	-	1

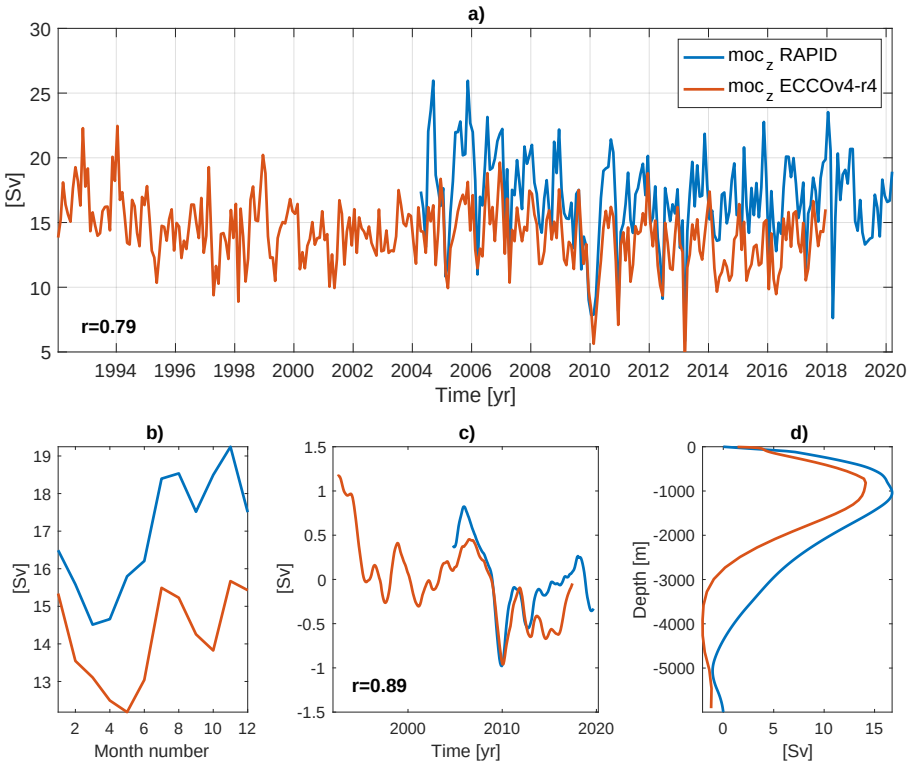

Figure S 1. Comparison between ECCOv4-r4 and observations at RAPID 26.5°N. (a) Monthly mean overturning strength (moc_z), and the (b) seasonal cycle, (c) interannual variability (normalized and 1-year low-pass filtered), (d) and climatological overturning stream function during 2004-2020 for observations and during 1992-2017 for ECCOv4-r4.

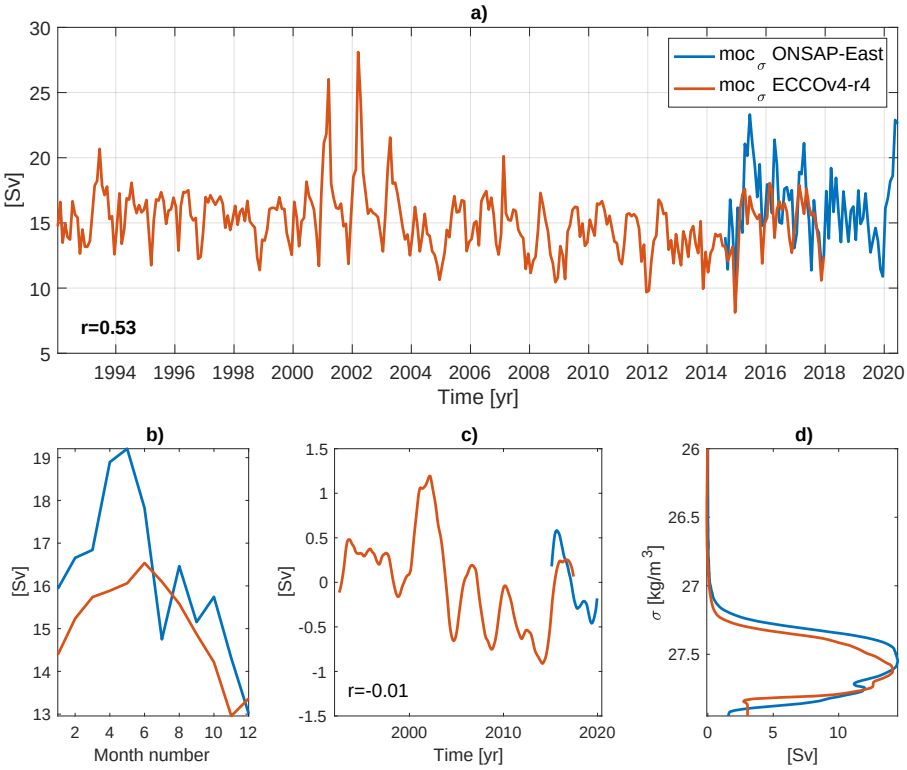

Figure S 2. Comparison between ECCOv4-r4 and observations at OSNAP-East. (a) Monthly mean overturning strength (moc_σ), and the (b) seasonal cycle, (c) interannual variability (normalized and 1-year low-pass filtered), and (d) climatological overturning stream function during 2014-2020 for observations and during 1992-2017 for ECCOv4-r4.

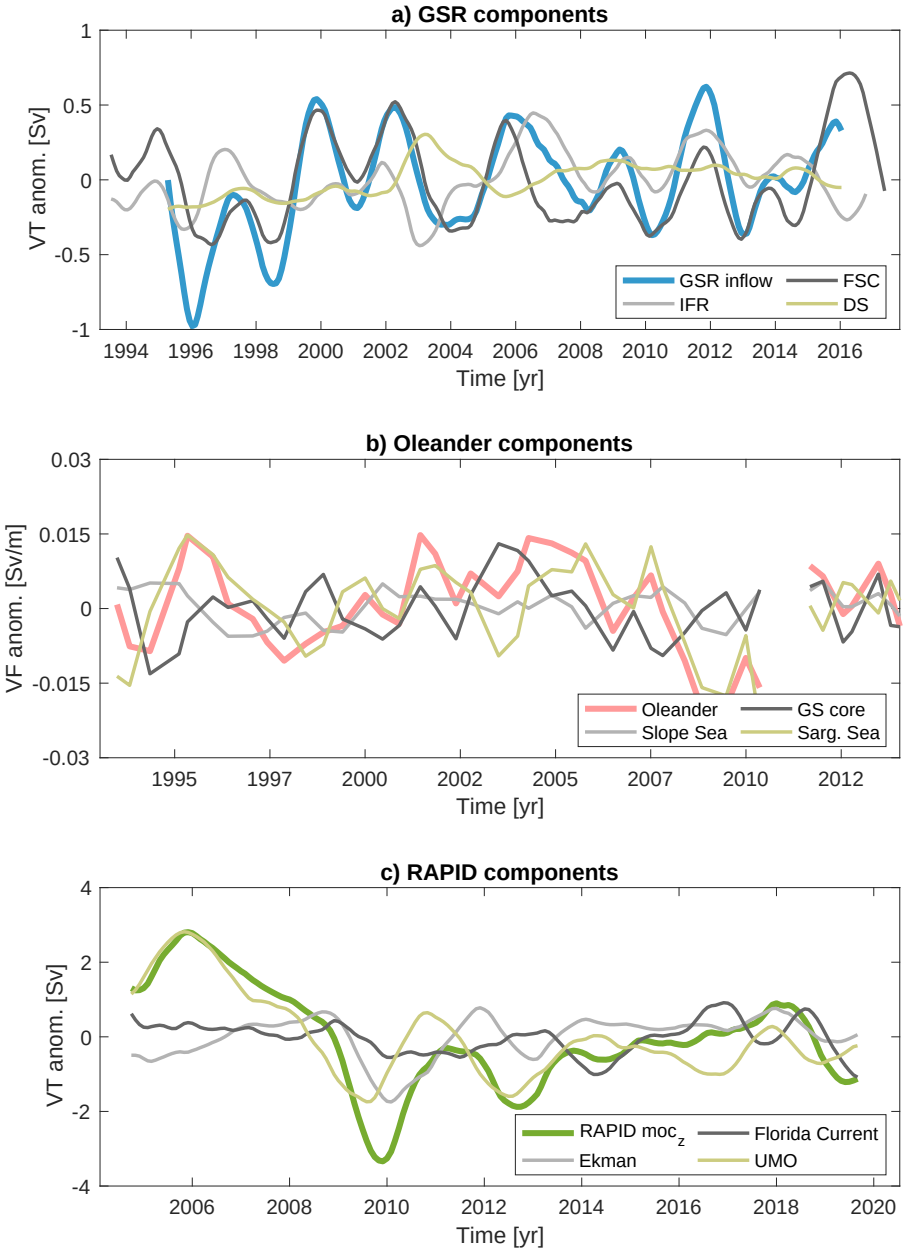

Figure S 3. Decomposition of observational transport records. Transport anomalies from the time-mean at a) the Greenland-Scotland Ridge (IFR; Iceland-Faroe Ridge, FSC; Faroe-Shetland Channel, DS; Denmark Strait), b) the Oleander section (Slope Sea, Gulf Stream core, Sargasso Sea), and c) the RAPID section (Ekman transport, Florida Current, UMO; Upper mid-ocean transport). The Oleander Gulf Stream core is the component used in the main analysis. Note that the Sargasso Sea and Slope Sea components at Oleander, and the UMO component at RAPID have a net southward transport.

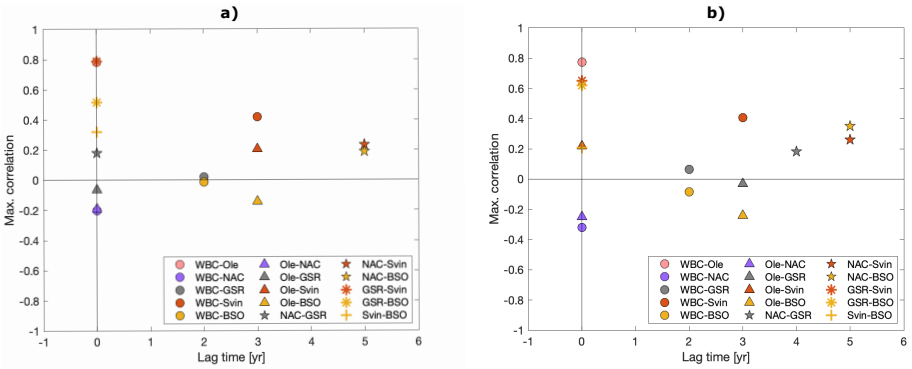

Figure S 4. Maximum correlation between the transport sections in ECCOv4-r4 within 0-6 year lag time. a) As in Table 3, only that maximum correlation with corresponding lag time is displayed. b) As in a), but with the Ekman layer (0-100m) removed from the section transports. The section name stated second in the legend lags the section name stated first.

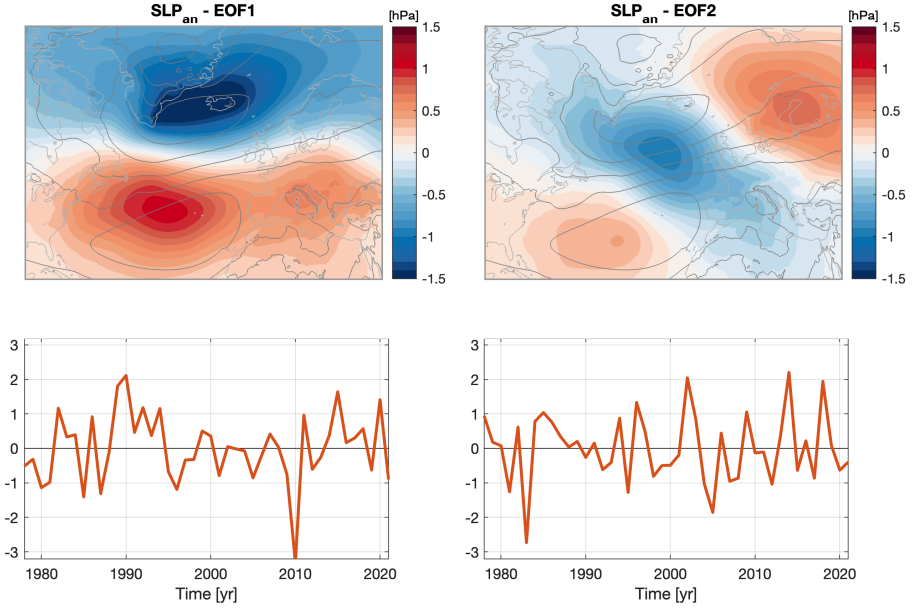

Figure S 5. The leading two EOF modes of North Atlantic (20-80°N, 90°W-40°E) annual mean sea level pressure (SLP) variability from ERA5 in color, and the associated principal component time series. EOF1 (NAO; North Atlantic Oscillation) explains 49% and EOF2 (EAP; East Atlantic Pattern) explains 15% of the variability. Grey contour lines show the climatological annual mean SLP pattern (contours plotted every 3 hPa from 1007 hPa to 1019 hPa). The climatological SLP centre in the north is the Icelandic low and the centre in the south is the Azores high.

Figure S 6. NAO and EAP indexes (as defined in Figure S5) accumulated over the 10 years prior.

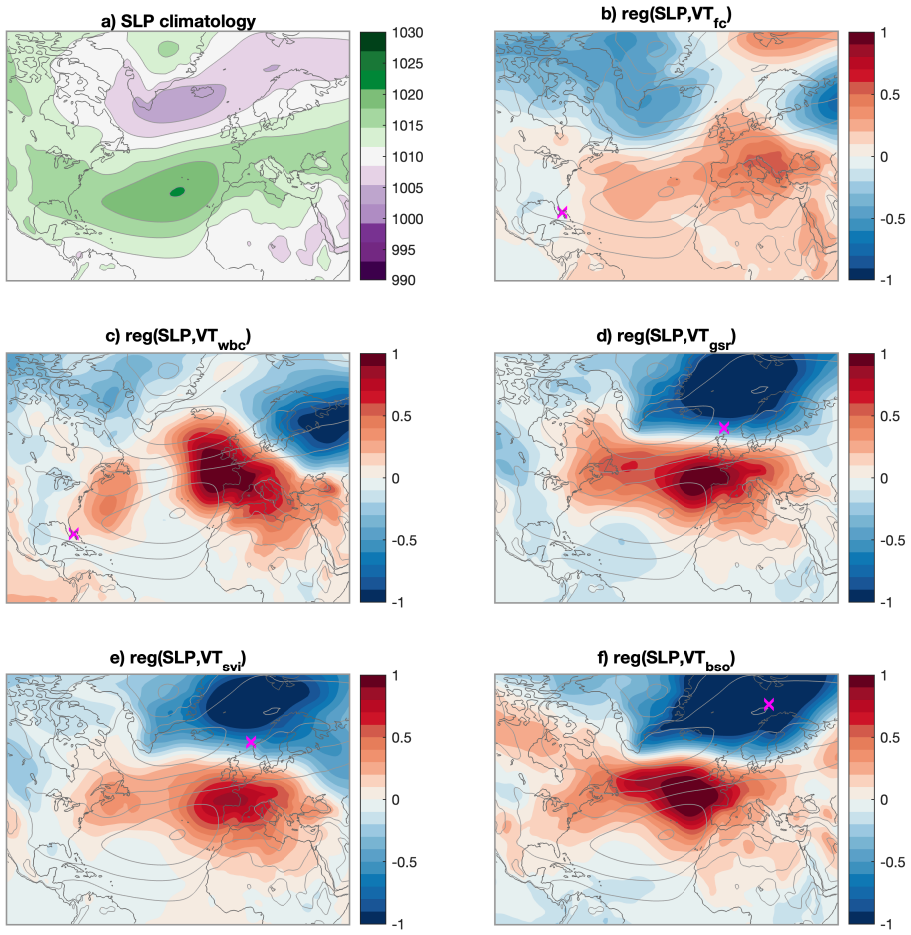

Figure S 7. Observed transport variability and large-scale atmospheric circulation patterns for comparison with ECCOv4-r4 (Figure S8). (a) ERA5 climatological sea level pressure (SLP; 1992-2017). ERA5 annual mean sea level pressure (hPa) regressed onto annual mean volume transport (VT; Sv) time series from observations; (b) Florida Current (1992-2017), (c) Western Boundary Current at 26.5^{o}N (wbc; 2005-2017), (d) Greenland-Scotland Ridge (gsr; 1995-2015), (e) NwASC at Svinøy (svi; 1996-2017), and (f) Barents Sea Opening inflow (bso; 1998-2016). Unit is hPa per standard deviation of volume transport. The volume transport time series has been normalized ($\frac{X-\mu_x}{\sigma_x}$) for comparable magnitudes between the panels. Gray contour lines show the climatological annual mean SLP pattern (contour interval: every 3 hPa from 1007 to 1019 hPa). The magenta cross marks the approximate location for the volume transport time series.

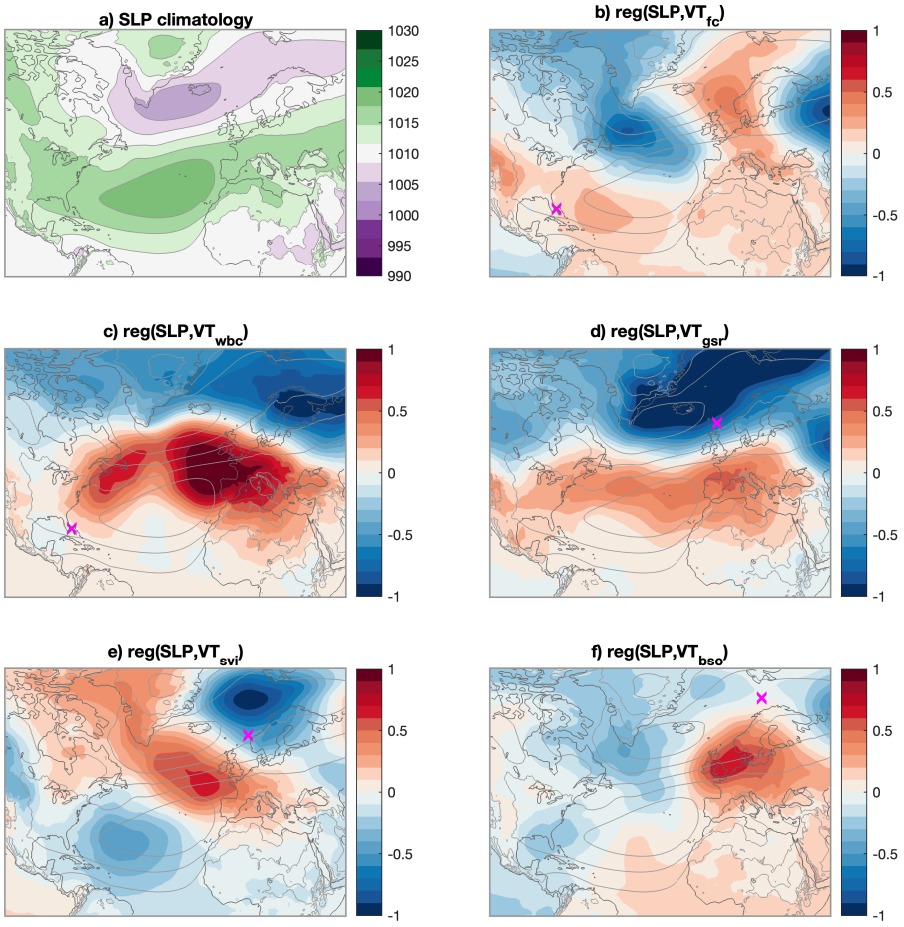

Figure S 8. ECCOv4-r4 transport variability and large-scale atmospheric circulation patterns for comparison with observations (Figure S7). (a) ECCOv4-r4 climatological sea level pressure (SLP; 1992-2017). Annual mean sea level pressure (hPa) regressed onto annual mean volume transport (VT; Sv) time series in ECCOv4-r4; (b) Florida Current (1992-2017), (c) Western Boundary Current at 26.5^{o}N (wbc; 2005-2017), (d) Greenland-Scotland Ridge (gsr; 1995-2015), (e) NwASC at Svinøy (svi; 1996-2017), and (f) Barents Sea Opening inflow (bso; 1998-2016). Unit is hPa per standard deviation of volume transport. The volume transport time series has been normalized ($\frac{X-\mu_x}{\sigma_x}$) for comparable magnitudes between the panels. Gray contour lines show the climatological annual mean SLP pattern (contour interval: every 3 hPa from 1007 to 1019 hPa). The magenta cross marks the approximate location for the volume transport time series.